

Organic–Organometallic Crystal Synthesis. 1. Hosting Paramagnetic $[(\eta^6\text{-Arene})_2\text{Cr}]^+$ (Arene = Benzene, Toluene) in Organic Anion Frameworks via O–H \cdots O and C–H \cdots O Hydrogen Bonds

Dario Braga,^{*,†} Anna Luisa Costa, Fabrizia Grepioni,^{*} Laura Scaccianoce, and Emilio Tagliavini^{*}

Dipartimento di Chimica G. Ciamician, Università di Bologna, Via Selmi 2, 40126 Bologna, Italy

Received May 21, 1996[⊗]

The engineering of organic–organometallic crystals based on hydrogen bonding and on shape complementarity is discussed. The crystalline salts $[(\eta^6\text{-C}_6\text{H}_6)_2\text{Cr}][(\text{CHD})_4]$ (**1**) and $[(\eta^6\text{-C}_6\text{H}_5\text{Me})_2\text{Cr}][(\text{CHD})_2]$ (**2**), in which the paramagnetic cations $[(\eta^6\text{-C}_6\text{H}_6)_2\text{Cr}]^+$ and $[(\eta^6\text{-C}_6\text{H}_5\text{Me})_2\text{Cr}]^+$ are encapsulated within organic anion frameworks derived from 1,3-cyclohexanedione (CHD), have been constructed. The idea of this *crystal synthesis* stems from the structure of the host–guest cyclamer $(\text{CHD})_6\cdot(\text{C}_6\text{H}_6)$ prepared by Etter et al. (*J. Am. Chem. Soc.* **1986**, *108*, 5871). The crystals are held together by O–H \cdots O hydrogen bonds between the supramolecular $[(\text{CHD})_2]^- \cdot (\text{CHD})_2$ and $[(\text{CHD})_2]^-$ anions and by C–H \cdots O hydrogen bonds between the anions and the organometallic cations. The hydrated crystalline species $[(\eta^6\text{-C}_6\text{H}_6)_2\text{Cr}][\text{OH}]\cdot 3\text{H}_2\text{O}$ (**3**) and $[(\eta^6\text{-C}_6\text{H}_6)_2\text{Cr}][\text{CHD}]\cdot 3\text{H}_2\text{O}$ (**4**) have also been prepared and structurally characterized. The crystals are held together by O–H \cdots O as well as C–H \cdots O interactions involving the water molecules. The hydroxide forms a polar crystal structure composed of an ABAB stacking sequence of layers containing OH $^-$ groups and water molecules and layers containing $[(\eta^6\text{-C}_6\text{H}_6)_2\text{Cr}]^+$ cations distributed in herringbone fashion.

Introduction

Crystal engineering is the planning of a crystal structure from its building blocks, molecules, or ions.¹ Since the interactions responsible for crystal cohesion are the same as those which hold together molecular aggregates in supermolecules, crystal engineering is logically connected to supramolecular chemistry.² Conceptually, the analogy between supramolecular chemistry and crystal engineering is stringent: the most representative process of molecular self-recognition and self-assembling is probably the very nucleation and growth of a molecular crystal from a solution or a melt.

Crystals are the most accessible systems for a detailed study of the geometric and energetic features of noncovalent interactions. Much of the current interest in studying intermolecular interactions in the solid state stems from the attraction represented by materials chemistry now at the forefront of solid state chemistry.³

The masterkey interaction to crystal engineering is undoubtedly hydrogen bonding,⁴ although anion–cation interactions⁵ as well as van der Waals interactions⁶ also take part in the recognition and aggregation processes

and determine the cohesion of the crystalline edifice. Hydrogen bonds of the O–H \cdots O, N–H \cdots O, and N–H \cdots N types are generally an order of magnitude stronger than van der Waals interactions and are directional.⁷ Strength and directionality allow *desk modeling* of supramolecular aggregates formed by molecules carrying adequately chosen donor and acceptor groups.⁸ This simple idea is being widely exploited, as witnessed by the number of excellent contributions from many different groups. Most of this work, however, is essentially in the domain of organic chemistry, which has seen the initial pioneering explorations, whereas solid state organometallic

(3) Some entry points: (a) Marks, T. J.; Ratner, M. A. *Angew. Chem., Int. Ed. Engl.* **1995**, *34*, 155. (b) Kanis, D. R.; Ratner, M. A.; Marks, T. J. *Chem. Rev.* **1994**, *94*, 195. (c) Miller, J. S.; Epstein, A. J.; Reiff, W. M. *Acc. Chem. Res.* **1988**, *21*, 114. (d) Gatteschi, D.; Pardi, L.; Sessoli, R. *Mater. Sci.* **1991**, *17*, 7. (e) Rouxel, J. *Acc. Chem. Res.* **1992**, *25*, 328. (f) Moore, J. S.; Lee, S. *Chem. Ind.* **1994**, 556. (g) Ghadiri, M. R.; Kobayashi, K.; Granja, J. R.; Chadha, R. K.; McRee, D. E. *Angew. Chem., Int. Ed. Engl.* **1995**, *34*, 93. (h) Etter, M. C. *Acc. Chem. Res.* **1990**, *23*, 120. (i) Braga, D.; Grepioni, F. *Acc. Chem. Res.* **1994**, *27*, 51. (4) (a) Jeffrey, G. A.; Saenger, W. *Hydrogen Bonding in Biological Structures*; Springer-Verlag: Berlin, 1991. (b) Jeffrey, G. A.; Maluszynska, H. *Acta Crystallogr., Sect. B* **1990**, *B46*, 546. (c) Bouquiere, J. P.; Finney, J. L. *Acta Crystallogr., Sect. B* **1994**, *B50*, 566.

(5) Braga, D.; Grepioni, F.; Milne, P.; Parisini, E. *J. Am. Chem. Soc.* **1993**, *115*, 5115.

(6) (a) Kitaigorodsky, A. I. *Molecular Crystals and Molecules*; Academic Press: New York, 1973. (b) Gavezzotti, A.; Filippini, G. *J. Am. Chem. Soc.* **1995**, *117*, 12299.

(7) (a) Bernstein, J.; Davis, R. E.; Shimoni, L.; Chang, N.-L. *Angew. Chem., Int. Ed. Engl.* **1995**, *34*, 1555. (b) Bernstein, J.; Leiserowitz, L. In *Structure Correlation*; Bürgi, H.-B., Dunitz, J. D., Eds.; VCH: Weinheim, 1994; Chapter 11, pp 431–500.

(8) (a) Desiraju, G. R. *Angew. Chem., Int. Ed. Engl.* **1995**, *34*, 2311. (b) Burrows, A. D.; Chan, C.-W.; Chowdry, M. M.; McGrady, J. E.; Mingos, D. M. P. *Chem. Soc. Rev.* **1995**, 329. (c) Subramanian, S.; Zaworotko, M. J. *Coord. Chem. Rev.* **1994**, *137*, 357. (d) Brammer, L.; Zhao, D.; Ladipo, F. T.; Braddock-Wilking, J. *Acta Crystallogr., Sect. B* **1995**, *B51*, 632.

[†] E-mail: DBRAGA@CIAM.UNIBO.IT. <http://catullo.ciam.unibo.it>.

[⊗] Abstract published in *Advance ACS Abstracts*, April 1, 1997.

(1) (a) Schmidt, G. M. J. *Pure Appl. Chem.* **1971**, *27*, 647. (b) Desiraju, G. R. *Crystal Engineering: The Design of Organic Solids*; Elsevier, Amsterdam, 1989. (c) Sharma, C. V. K.; Desiraju, G. R. In *Perspectives in Supramolecular Chemistry. The Crystal as a Supramolecular Entity*; Desiraju, G. D., Ed.; Wiley: New York, 1996.

(2) (a) Lehn, J.-M.; Mascal, M.; Fisher, J. J. *Chem. Soc., Chem. Commun.* **1990**, 479. (b) Whitesides, G. M.; Simanek, E. E.; Mathias, J. P.; Seto, C. T.; Chin, D. N.; Mammen, M.; Gordon, D. M. *Acc. Chem. Res.* **1995**, *28*, 37. (c) Etter, M. C. *J. Am. Chem. Soc.* **1982**, *104*, 1095.

chemistry is still a mostly uncharted territory.⁹ Hydrogen bonding in organometallic crystals has only recently begun to be investigated in a systematic manner.¹⁰

Organometallic chemistry is the perfect ambient to develop supramolecular aggregate systems because organometallic molecules combine the intra- and intermolecular bonding features of organic fragments (the ligands) with the variable valence state and magnetic behavior of transition metal atoms.⁹

In this article, we describe the results of our efforts to synthesize and structurally characterize organic–organometallic crystals. In devising this work, we have made use of two basic concepts of molecular modeling: (i) the “shape analogy” between organic molecules and those organometallic molecules which carry the same organic fragments as ligands¹¹ and (ii) the complementary roles of strong and directional hydrogen bonds (such as O–H···O), which link selectively and tightly organic molecules, and of diffuse networks of weak C–H···O hydrogen bonds and anion–cation interactions, which link the organic and organometallic fragments in the crystal.^{12,13}

The organic–organometallic shape analogy concept is chiefly the recognition that solid state interactions between molecules or ions are governed by the type and distribution of peripheral atoms with marginal contribution from the atoms “inside”, which are screened from the surrounding. Hence, *molecules with similar shape and size are organized in the solid state in similar manner, irrespective of the chemical composition.* A good example of “shape analogy” is afforded by the close similarity between the crystal structures of benzene and bis(benzene)chromium.¹¹ Both crystal structures are based on herringbone patterns that allow C–H···ring interactions to be maximized. It has been recently pointed out that the supramolecular concept is effectively a bridge between organic, inorganic, and organometallic crystal chemistry.¹⁴

The second synthetic idea stems from the recognition that C–H···O interactions, though “soft” in comparison to hard O–H···O and N–H···O bonds, are important for crystal cohesion because of the profusion of C–H donors carried by the ligands in organometallic molecules and of acceptors, such the CO ligand in its various modes of bonding.^{10c,13} The benzene ligand, for example, is potentially a six-fold C–H donor. It will be shown below that this feature can be utilized in desk planning of crystal structures.

Given these conceptual premises, it will be immediately clear why we have chosen to investigate the interaction between a well-studied cyclic dione, 1,3-cyclohexanedione (CHD), and a prototypical organometallic molecule, the sandwich molecule bis(benzene)chromium, (η^6 -C₆H₆)₂Cr. The hydrogen-bonding char-

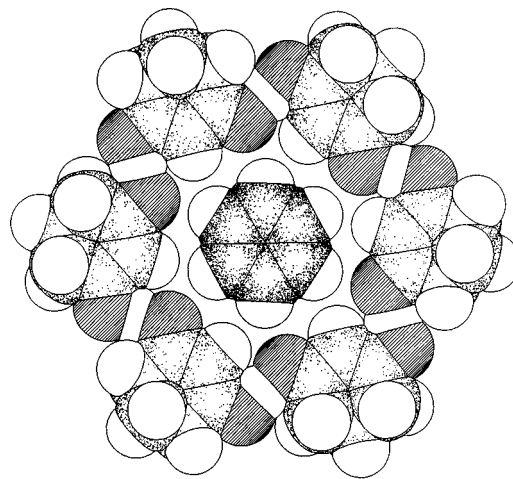


Figure 1. Etter's 1,3-cyclohexanedione [CHD]₆ cyclamer encapsulating benzene. Dashed atoms represent the oxygen atoms.

acteristics of diones have also been extensively studied and constitute the basis of the resonance-assisted hydrogen bond model (RAHB).¹⁵

1,3-Cyclohexanedione (CHD) was shown by Etter to crystallize in two crystalline forms:¹⁶ one containing chains of molecules linked head-to-tail via O–H···O=C hydrogen bonds [O···O distance, 2.561(4) Å] and one in which six CHD molecules form a ring (a cyclamer) which encloses an ordered benzene molecule. In this latter form, the CHD molecules adopt a *syn–anti* hydrogen-bonding configuration with respect to the orientation of the OH group and of the hydrogen bond involving the carbonyl group. In such a way, the “free” carbonyl lone pair points toward the encapsulated benzene molecule. The O···O separation is slightly longer than that in the chain form [2.579(1) Å]. Since it bears on the following discussion, the structure of Etter's cyclamer is shown in Figure 1.

In this article, we will show that crystalline products related to Etter's cyclamer can, indeed, be synthesized when the neutral sandwich molecules (η^6 -C₆H₆)₂Cr and (η^6 -C₆H₅Me)₂Cr are oxidized to the corresponding Cr(I) complexes by molecular oxygen in the presence of CHD in THF or other solvents.¹⁷ Crystallization from anhydrous THF allows the preparation and characterization by single-crystal X-ray diffraction of the organic–organometallic crystals [η^6 -C₆H₆)₂Cr][CHD]₄ (**1**)¹⁷ and [η^6 -C₆H₅Me)₂Cr][CHD]₂ (**2**). In the presence of water, the hydrated hydroxide [η^6 -C₆H₆)₂Cr][OH]·3H₂O (**3**) and the mixed system [η^6 -C₆H₆)₂Cr] [CHD]·3H₂O (**4**) have also been obtained and characterized.¹⁸ The hydrogen bonding patterns within the supramolecular organic moieties as well as between organic and organometallic units will be discussed in detail. The participation of water in the patterns of O–H···O and C–H···O interactions involving the bis-arene complexes **3** and **4** will also be described. The analogy between

(9) Braga, D.; Grepioni, F. *J. Chem. Soc., Chem. Commun.* **1996**, 571.

(10) (a) Braga, D.; Grepioni, F.; Sabatino, P.; Desiraju, G. R. *Organometallics* **1994**, *13*, 3532. (b) Biradha, K.; Desiraju, G. R.; Braga, D.; Grepioni, F. *Organometallics* **1996**, *15*, 2692. (c) Braga, D.; Biradha, K.; Grepioni, F.; Pedireddi, V. R.; Desiraju, G. R. *J. Am. Chem. Soc.* **1995**, *117*, 3156. (d) Braga, D.; Grepioni, F.; Tedesco, E.; Desiraju, G. R.; Biradha, K. *Organometallics* **1996**, *15*, 1284.

(11) Braga, D.; Grepioni, F. *Organometallics* **1991**, *10*, 2563.

(12) Braga, D.; Byrne, J. J.; Calhorda, M. J.; Grepioni, F. *J. Chem. Soc., Dalton Trans.* **1995**, 3287 and references therein.

(13) Braga, D.; Grepioni, F. *Acc. Chem. Res.* **1997**, *30*, 81.

(14) Desiraju, G. R. *J. Mol. Struct.* **1996**, *374*, 191.

(15) (a) Gilli, G.; Bellucci, F.; Ferretti, V.; Bertolasi, V. *J. Am. Chem. Soc.* **1989**, *111*, 1023. (b) Bertolasi, V.; Gilli, P.; Ferretti, V.; Gilli, G. *J. Am. Chem. Soc.* **1991**, *113*, 4917. (c) Gilli, G.; Bertolasi, V.; Ferretti, V.; Gilli, P. *Acta Crystallogr., Sect. B* **1993**, *B49*, 564.

(16) Etter, M. C.; Urbonczyk-Lipkowska, Z.; Jahn, D. A.; Frye, J. S. *J. Am. Chem. Soc.* **1986**, *108*, 5871.

(17) Braga, D.; Grepioni, F.; Byrne, J. J.; Wolf, A. *J. Chem. Soc., Chem. Commun.* **1995**, 1023.

(18) Braga, D.; Costa, A. L.; Grepioni, F.; Scaccianocce, L.; Tagliavini, E. *Organometallics* **1996**, *15*, 1084.

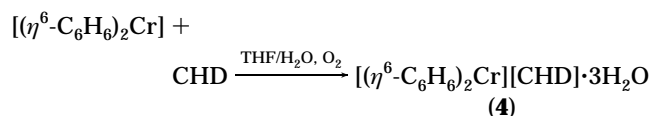
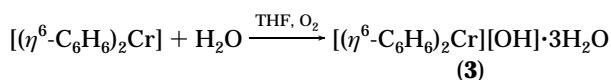
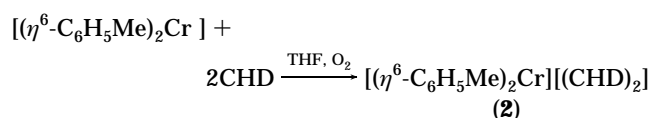
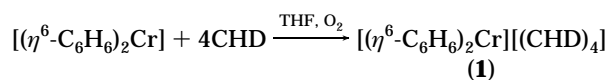
the water–OH[−] layer structure in **3** and that of ice will be discussed.

Synthesis and Characterization

When neutral (η^6 -C₆H₆)₂Cr and (η^6 -C₆H₅Me)₂Cr are reacted with CHD in THF solution, a redox process occurs, yielding the paramagnetic cations [(η^6 -C₆H₆)₂Cr]⁺ and [(η^6 -C₆H₅Me)₂Cr]⁺. The oxidant is very likely O₂ present in traces in the solvent. The reaction may involve formation of O₂[−] or O₂^{•−}, which are then capable of abstracting H⁺ from the fairly acidic dione, thus producing in situ CHD[−] and water in stoichiometric quantities (see also below).

[(η^6 -C₆H₆)₂Cr] was purchased from Strem, while [(η^6 -C₆H₅Me)₂Cr] was synthesized according to the procedure suggested by Calderazzo et al.¹⁹ based on a modification of the original synthesis by Fisher et al.²⁰ Both complexes, once prepared, were sealed in vials under argon.

The crystal syntheses are summarized in the following scheme:



Synthesis of Crystalline [(η^6 -C₆H₆)₂Cr][CHD]₄ (1). White powder of CHD (400 mg, 3.6 mmol) and brown crystalline (η^6 -C₆H₆)₂Cr (125 mg, 0.60 mmol) were added to a dry Schlenk tube and ground with a glass rod under argon atmosphere. The finely ground mixture was then dried in vacuo (1 h) to remove any water present in solid CHD. Anhydrous THF (30 mL) was then added to the mixture. The mixture was stirred until complete dissolution. Deep yellow crystals, stable in the air, were obtained by slow evaporation of the solvent at 0 °C. Unambiguous characterization of the chromium complex as the paramagnetic cation [(η^6 -C₆H₆)₂Cr]⁺ was obtained from the solution ¹H NMR spectrum which revealed four very broad resonances of the CHD[−] moiety [δ 5.86, 3.44, 2.41, and 2.00 ppm relative to CDCl₃ as internal standard at δ 7.2716 ppm], indicating the presence in solution of paramagnetic material, consistent with the formulation as a Cr(I) salt. No resonance of the aromatic ligand was observed.

Synthesis of Crystalline [(η^6 -C₆H₅Me)₂Cr][CHD]₂ (2). Bistoluene chromium (150 mg, 0.6 mmol) and THF (10 mL) were stirred under Ar at room temperature for 15 min, and then the solution was filtered under Ar to remove some insoluble black material. CHD (400 mg, 0.46 mmol) was added to the clear brown solution and stirring was continued until complete dissolution. Cooling at 0 °C and slow evaporation of the solvent afforded bright yellow crystals suitable for X-ray diffraction.

Synthesis of Crystalline [(η^6 -C₆H₆)₂Cr][OH]·3H₂O (3). [(η^6 -C₆H₆)₂Cr] (0.10 g, 0.48 mmol) was dissolved in benzene (20 mL). Water (19 mL) was added and oxygen bubbled

through the two-layer system until the benzene layer was almost colorless. The yellow water layer was separated and concentrated to dryness in vacuo. The solid residue was dissolved in a small amount of CHCl₃ and transferred to a flask under Ar. Slow evaporation of the solvent afforded crystals suitable for X-ray diffraction.

Synthesis of Crystalline [(η^6 -C₆H₆)₂Cr][CHD]·3H₂O (4). Air was bubbled through a brown solution of [(η^6 -C₆H₆)₂Cr] (0.10 g, 0.48 mmol) in 9:1 THF/H₂O (30 mL) and CHD (0.056 g, 0.50 mmol) until the brown color turned to yellow. The reaction mixture was stirred at room temperature for 30 min and then filtered to remove some green material (probably some Cr(III) compound coming from overoxidation) and concentrated to dryness in vacuo. The solid residue was dissolved in a small amount of THF and transferred to a flask connected to an Ar line.

Slow evaporation of the solvent afforded bright yellow crystals suitable for X-ray diffraction. In solution and at room temperature, both **3** and **4** slowly oxidize in the air to unidentified green material.

The NMR spectra were recorded on a Varian Gemini 300 instrument at 300 MHz in CDCl₃. 1,3-Cyclohexanedione was purchased from Aldrich. THF was distilled from sodium benzophenone ketyl and CHCl₃ from P₂O₅ and was stored under argon. All the reactions were carried under argon atmosphere in oven-dried glassware.

Crystal Structure Characterization. All X-ray diffraction data collections were carried out on a Nonius CAD-4 diffractometer equipped with a Nonius liquid N₂ low-temperature device. Data were collected at room temperature (approximately 293 K) for **1**, **3**, and **4** and at both room temperature and 223 K for **2**. Crystal data and details of measurements are reported in Table 1. Diffraction data were corrected for absorption by azimuthal scanning of high- γ reflections. SHELX86^{21a} and SHELXL92^{21b} were used for structure solution and refinement based on *F*². Fractional atomic coordinates and anisotropic displacement parameters are deposited as Supporting Information. SCHAKAL93 was used for the graphical representation of the results.^{22a} The computer program PLATON^{22b} was used to analyze the geometry of the hydrogen bonding patterns. All non-H atoms were allowed to vibrate anisotropically. Methylenic hydrogen atoms of the CHD molecules were added in calculated positions (C–H, 0.97 Å) for **1–4**. Calculated positions were also used for the remaining hydrogen atoms in **2–4** (C–H, 0.93 Å), while benzene hydrogen atoms were directly located from low- θ (<20°) Fourier maps in **1**. In all cases, hydrogen atom isotropic thermal parameters were refined on the basis of the corresponding C atoms [*U*(H) = 1.2*U*_{eq}(C)]. A careful analysis of the anisotropic displacement parameters of the CHD atoms in **1** revealed the presence of disorder due to the twisted conformation of the CHD rings (an ORTEP drawing of the system is available as Supporting Information). Two of the four systems present an unusually flat geometry due to the averaging of the two possible out-of-plane positions of the outermost CH₂ groups. Attempts to refine separately the two alternative positions were unsuccessful because of the close proximity of the two electron density peaks in spite of the good data resolution ($2\theta_{\text{max}} = 60^\circ$ in the case of **1**). Final refinements were, therefore, carried out on a disorder model based on an average of the two positions convoluted in a large anisotropy perpendicular to the plane of the CHD. As a consequence, the short C–C bond lengths involving the outermost CH₂ systems are an artifact of the disorder model and will not be used in the structural comparison.

(21) (a) Sheldrick, G. M. *Acta Crystallogr., Sect. A* **1990**, *A46*, 467. (b) Sheldrick, G. M. *SHELXL92, Program for Crystal Structure Determination*; University of Göttingen: Göttingen, Germany, 1993. (22) (a) Keller, E. *SCHAKAL93, Graphical Representation of Molecular Models*; University of Freiburg: Freiburg, Germany, 1993. (b) Spek, A. L. *Acta Crystallogr., Sect. A* **1990**, *A46*, C31.

(19) Calderazzo, F.; Invernizzi, R.; Marchetti, F.; Masi, F.; Moalli, A.; Pampaloni, G.; Rocchi, L. *Gazz. Chim. It.* **1993**, *123*, 53.

(20) (a) Fisher, E. O.; Hafner, W. *Z. Anorg. Allg. Chem.* **1957**, *79*, 3062. (b) Tsutsui, M.; Chang, G. *Can. J. Chem.* **1963**, *41*, 1255.

Table 1. Crystal Data and Details of Measurements for Crystals 1, 2a,b, 3, and 4

	1	2a	2b	3	4
formula	C ₃₆ H ₄₃ CrO ₈	C ₂₄ H ₂₀ CrO ₂	C ₂₄ H ₂₀ CrO ₂	C ₁₂ H ₁₉ CrO ₄	C ₁₈ H ₁₉ CrO ₅
mol wt	656.71	392.40	392.40	279.27	367.33
temp (K)	293(2)	293(2)	223(2)	293(2)	293(2)
system	triclinic	orthorhombic	orthorhombic	orthorhombic	orthorhombic
space group	<i>P</i> $\bar{1}$	<i>Pbcn</i>	<i>Pbcn</i>	<i>Aba2</i>	<i>Pbca</i>
<i>a</i> (Å)	8.113(2)	6.945(2)	6.898(3)	7.825(3)	7.948(2)
<i>b</i> (Å)	13.000(7)	21.589(5)	21.430(5)	10.506(4)	16.919(8)
<i>c</i> (Å)	17.121(3)	15.255(6)	15.22(2)	16.409(5)	26.547(6)
α (deg)	109.63(3)	90	90	90	90
β (deg)	99.890(10)	90	90	90	90
γ (deg)	98.16(2)	90	90	90	90
<i>V</i> (Å ³)	1636.3(10)	2287.3(12)	2250(3)	1349.0(8)	3570(2)
<i>F</i> (000)	696	816	816	588	1528
λ (Mo K α) (Å)	0.71073	0.71073	0.71073	0.71073	0.71073
transmission coeffs (min–max)	0.91–1.00	0.85–1.00	0.85–1.00	0.87–1.00	0.78–1.00
μ (Mo K α) (mm ⁻¹)	0.401	0.513	0.522	0.848	0.664
θ range (deg)	3.0–30.0	3.0–25.0	3.0–28.0	3.5–25.0	3.0–25.0
octants explored					
<i>h</i> _{min} / <i>h</i> _{max}	–11 < <i>h</i> < 11	0 < <i>h</i> < 8	0 < <i>h</i> < 9	0 < <i>h</i> < 9	0 < <i>h</i> < 9
<i>k</i> _{min} / <i>k</i> _{max}	–18 < <i>k</i> < 17	0 < <i>k</i> < 25	0 < <i>k</i> < 28	0 < <i>k</i> < 12	0 < <i>k</i> < 20
<i>l</i> _{min} / <i>l</i> _{max}	0 < <i>l</i> < 24	0 < <i>l</i> < 18	0 < <i>l</i> < 21	0 < <i>l</i> < 19	0 < <i>l</i> < 30
measd reflns	9795	2393	3067	698	3571
unique reflns	9490	2039	2734	607	3116
no. of refined params	454	181	181	79	212
GOF on <i>F</i> ²	1.382	1.053	1.053	1.130	1.081
R1 (on <i>F</i> , <i>I</i> > 2 σ (<i>I</i>))	0.0525	0.0388	0.0738	0.0376	0.0599
wR2 (on <i>F</i> ² , all data)	0.1863	0.1256	0.2592	0.1236	0.2088

The same type of disorder may also affect the central CH₂ system in **4**.

To evaluate the C–H(benzene)⋯O(CHD) bond lengths, all C–H(benzene) distances were normalized along the experimentally observed direction to the neutron-derived value of 1.08 Å.

Results and Discussion

Although the main focus of this paper is on the hydrogen bonding and supramolecular organization in crystalline [(η^6 -C₆H₆)₂Cr][(CHD)₄] (**1**), [(η^6 -C₆H₅Me)₂Cr]–[(CHD)₂] (**2**), [(η^6 -C₆H₆)₂Cr][OH]·3H₂O (**3**), and [(η^6 -C₆H₆)₂Cr][CHD]·3H₂O (**4**), it is worthwhile to briefly discuss the structures of the two bis-arene cations, since the structural chemistry of bis-arene complexes of their type has not been extensively studied.²³ Relevant structural parameters relative to the three independent determinations of the [(η^6 -C₆H₆)₂Cr]⁺ cation and to that of the [(η^6 -C₆H₅Me)₂Cr]⁺ cation are reported in Table 2. Table 3 reports a comparison of bond lengths and angles within the CHD systems in **1**, **2**, and **4** (see Chart 1) and between these and the two determinations of crystalline CHD. Intermolecular hydrogen-bonding parameters calculated on normalized C–H and O–H distances are listed in Table 4. Estimated standard deviations are given in parentheses, while standard errors on average values are given as subscripts.

The key geometrical features of the two paramagnetic cations can be summarized as follows:

(i) The asymmetric units of crystalline **1** and **4** contains fully independent [(η^6 -C₆H₆)₂Cr]⁺ cations, with the benzene ligands adopting an eclipsed conformation.

(ii) In **3**, the chromium atom is on a crystallographic two-fold axis and one C₆H₆ ring is in a general position; hence, the eclipsed conformation is imposed by symmetry.

(iii) Cr–C bond lengths are strictly comparable in their mean values in the three bis-benzene complexes (2.137₆, 2.13₂, and 2.131₈ Å in **1**, **3**, and **4**, respectively) as well as in their ranges.

(iv) C–C bond distances are known with less accuracy, and the individual values are all similar within standard deviations. No significant pattern of long–short C–C bond length alternation can be detected.

(v) The benzene hydrogen atoms in **1** are found to bend *toward* the metal atom, with an average deviation (calculated on observed H atom positions) from the planes of the two rings of 0.10₂ and 0.07₂ Å.

(vi) The bis-toluene complex in crystalline **2** is disordered. The toluene ligands in the sandwich have the methyl groups in different relative conformations: in conformation A they are at 120° in projection, and in conformation B the Me groups are *trans* in projection with respect to the metal atom, as shown in Figure 2. The *trans*-eclipsed conformation, in which the methyl groups are on opposite sides of two eclipsed C₆ rings, has also been observed in the structures of [(η^6 -C₆H₅-Me)₂Cr]⁺I[–] ^{24a} and -Cl[–].^{24b} The disorder in **2** can be rationalized in terms of the intermolecular interactions with the [CHD₂][–] anion, as will be discussed below. Because of the disorder, the C₆ rings were refined with geometric constraints.

Before discussing the crystal architectures, it is worthwhile to briefly discuss the synthetic paths leading to **1–4**. We have not carried out any mechanistic investigation, but we can put forward some hypotheses. For **3** and **4**, the electron acceptor for the oxidation of the Cr(0) starting complexes to Cr(I) is certainly molecular oxygen, bubbled through the solution, which is reduced to superoxide radical anion (eq 1).^{25a} The latter is protonated by the acidic CHD if present (eq 2), or by water (eq 3), to give a HO₂[•] radical. Further reduction from a second (η^6 -Ar)₂Cr molecule and proton exchange

(23) Miller, J. S.; O'Hare, D. M.; Chakraborty, A.; Epstein, A. J. *J. Am. Chem. Soc.* **1989**, *111*, 7853. Morosin, B. *Acta Crystallogr., Sect. B* **1974**, *B30*, 838. Elschenbroich, C.; Gondrum, R. *Massa, W. Angew. Chem., Int. Ed. Engl.* **1985**, *24*, 967.

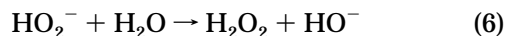
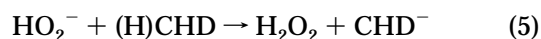
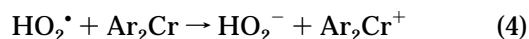
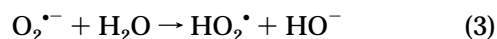
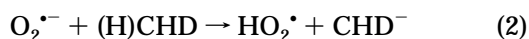
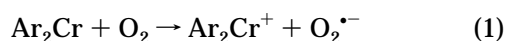
(24) (a) Starovskii, C. V.; Struchkov, Yu. T. *Zh. Strukt. Khim.* **1961**, *2*, 161. (b) Braga, D.; Costa, A. L.; Grepioni, F.; Tagliavini, E. Unpublished results.

Table 2. Comparison of Bond Distances (Å) for the $[(\eta^6\text{-C}_6\text{H}_6)_2\text{Cr}]^+$ Cation in **1**, **3**, and **4** and for the $[(\eta^6\text{-C}_6\text{H}_5\text{Me})_2\text{Cr}]^+$ Cation in **2a** and **2b**

system	1	2a (293 K)	2b (223 K)	3	4	
Cr–C	2.142(4)	2.205(5) ^a	2.228(6) ^a	2.147(14)	2.144(7)	
	2.128(4)	2.130(7) ^a	2.160(8) ^a	2.13(2)	2.131(6)	
	2.126(4)	2.053(8) ^a	2.067(8) ^a	2.114(14)	2.124(7)	
	2.144(4)	2.054(7) ^a	2.043(7) ^a	2.16(2)	2.114(7)	
	2.133(4)	2.131(6) ^a	2.115(6) ^a	2.10(2)	2.118(7)	
	2.135(4)	2.205(5) ^a	2.206(5) ^a	2.146(12)	2.129(7)	
	2.145(4)	2.076(7) ^b	2.048(7) ^b		2.152(7)	
	2.133(4)	2.161(7) ^b	2.145(7) ^b		2.125(6)	
	2.138(4)	2.221(6) ^b	2.231(5) ^b		2.116(7)	
	2.137(4)	2.200(6) ^b	2.224(5) ^b		2.130(7)	
	2.144(4)	2.116(7) ^b	2.130(6) ^b		2.126(7)	
	2.136(4)	2.052(6) ^b	2.040(6) ^b		2.137(7)	
	mean Cr–C ^c	2.137 ₆	2.135 ₃	2.136 ₄	2.13 ₂	2.129 ₁₁
	C(ring)–C(ring)	1.398(6)			1.364(13)	1.398(10)
		1.415(5)			1.397(8)	1.399(10)
1.388(6)				1.407(14)	1.380(10)	
1.397(5)				1.376(14)	1.378(11)	
1.393(6)				1.489(9)	1.396(11)	
1.392(5)				1.439(14)	1.396(11)	
1.397(6)					1.353(10)	
1.401(6)					1.376(12)	
1.405(5)					1.402(11)	
1.404(5)					1.367(12)	
1.392(5)					1.399(10)	
1.388(6)					1.390(9)	
mean		1.398 ₈			1.41 ₄	1.386 ₁₅
C(ring)–C(ring) ^c						
C(ring)–C(methyl)			A, 1.543(7)	A, 1.509(8)		
		B, 1.541(7)	B, 1.529(9)			

^a Conformer A. ^b Conformer B. ^c Subscripts represent standard errors on the mean values. ^d Because of the presence of disorder (see text), the C₆ rings were refined as rigid groups.

affords the stable hydrogen peroxide (eqs 4–6). The redox potentials of the species involved are in agreement with such a process.^{25b} Thus, two Ar₂Cr–CHD or Ar₂Cr–OH ion pairs are formed per molecule of oxygen consumed; this number could be doubled if a redox process between H₂O₂ and Ar₂Cr were active. In the formation of **1** and **2**, we believe that traces of oxygen present in the solvent, or accidentally introduced during manipulation, can account for the same kind of process depicted in eqs 1–6. Indeed, crystalline **4** can also be obtained by reacting sodium enolate (Na–CHD) with the hydroxide **3** in methanol solution.^{24c} However, an alternative mechanism involving direct electron transfer between neutral $(\eta^6\text{-Ar})_2\text{Cr}$ and CHD with the eventual formation of hydrogen cannot be confidently ruled out.

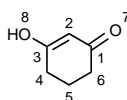


We can now proceed with a discussion of the ion organization in crystalline **1**–**4**. Crystal **1** was obtained first. The cation $[(\eta^6\text{-C}_6\text{H}_6)_2\text{Cr}]^+$ is trapped within the

“horseshoe”-shaped tetrameric monoanion in which the CHD units are linked via C=O⋯HO hydrogen bonds: O1⋯O4, 2.544(2); O6⋯O7, 2.570(2); and O2⋯O5, 2.469(2) Å (see Figure 3a). The two outer CHD molecules are in the keto-enol form, with the enol oxygens (O4 and O7) acting as hydrogen-bonding donors toward the inner tautomeric anion composed of one CHD molecule and one enolate group (see Table 3). The tautomeric pair is linked via O2 and O5. A final Fourier map showed the presence of a peak almost midway between O2 and O5 [O(2)⋯H(100) 1.24(1) Å; O(5)⋯H(100), 1.23(1) Å; O(2)⋯H(100)⋯O(5), 171(3)°], which can be attributed to an unresolved position of the unique hydrogen atom in the O⋯O hydrogen bond. The monoanion aggregate wraps around a single $[(\eta^6\text{-C}_6\text{H}_6)_2\text{Cr}]^+$ ion, as shown in Figure 3a. The interaction between the $[(\text{CHD})_4]^-$ tetramer and $[(\eta^6\text{-C}_6\text{H}_6)_2\text{Cr}]^+$ is based on C–H⋯O=C bonds: 10 benzene hydrogens per cation are involved in interactions in the range 2.29–2.70 Å, five contacts being shorter than 2.5 Å. The ion pairing very likely accounts for these short values.

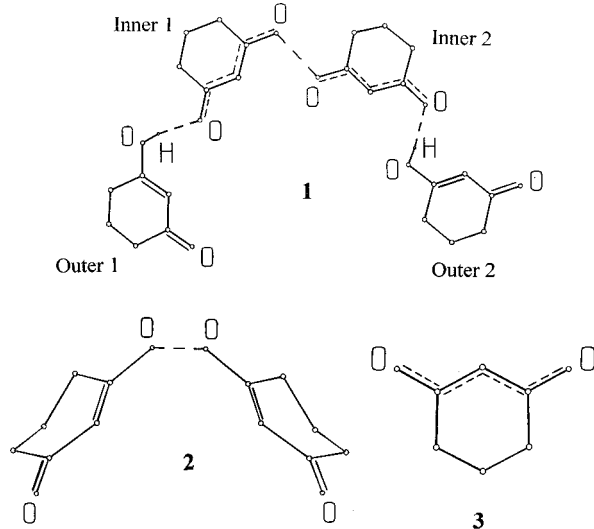
Two $[(\eta^6\text{-C}_6\text{H}_6)_2\text{Cr}][(\text{CHD})_4]$ systems are related by a center of inversion so that the C=O terminus (O8) links two $[(\eta^6\text{-C}_6\text{H}_6)_2\text{Cr}]^+$ cations via a bifurcated interaction.

(25) (a) The oxidation of Ar₂Cr to Ar₂Cr⁺ is a well-documented process: Fischer, E. O. *Inorg. Synth* **1960**, *6*, 132. (b) The redox standard potentials $E_{1/2}$ for the O₂/HO₂[•] pair in water is –0.125 V, while that of the O₂/H₂O₂ pair is 1.51 V: Bard, A. J.; Parson, R.; Jordan, J. *Standard Potentials in Water Solutions*; Marcel Dekker: New York, 1985; Chapter 4. The redox potential of the $(\eta^6\text{-C}_6\text{H}_6)_2\text{Cr}/(\eta^6\text{-C}_6\text{H}_6)_2\text{Cr}^+$ pair is –0.81 V in 8:2 MeOH/C₆D₆ vs SCE: Furlani, C.; Fischer, E. O. *Z. Elektrochem.* **1957**, *61*, 481. It shifts to –0.72 V vs SCE in DME: Vites, J. C.; Steffey, B. D.; Giuseppetti-Dery M. E.; Cutler, A. R. *Organometallics* **1991**, *10*, 2827. (c) The formation of the ion-pairing $(\eta^6\text{-Ar})_2\text{Cr}^+/\text{CHD}^-$ is, anyway, the keystone of the process: **4** can also be obtained from independently prepared solutions of sodium cyclohexanedionate [CHD[–]Na⁺] and $(\eta^6\text{-C}_6\text{H}_6)_2\text{Cr}^+\text{OH}^-(\text{H}_2\text{O})_n$.

Table 3. Comparison of Relevant Geometric Parameters (Distances, Å) between the CHD Systems in 1, 2, and 4 and in the Crystal Structures of CHD

	1–2	2–3 (C=C)	3–4	4–5	5–6	1–6	1–7 (C=O)	3–8 (C–OH)
CHD ¹⁶	1.409(5)	1.345(5)	1.483(5)	1.49(1)	1.43(1)	1.490(6)	1.243(2)	1.323(4)
[(CHD) ₆][C ₆ H ₆] ¹⁶	1.413(2)	1.349(2)	1.490(2)	1.512(2)	1.513(2)	1.495(2)	1.253(2)	1.318(2)
(CHD) ^{−,34} I	1.393(7)	1.396(4)	1.512 ^a	1.501 ^a	1.498 ^a	1.512 ^a	1.263(3)	1.268(3)
(CHD) ^{−,34} II	1.393(3)	1.409(8)	1.497 ^a	1.510 ^a	1.505 ^a	1.511 ^a	1.262(6)	1.263(7)
1								
inner 1	1.389(4)	1.360(4)	1.495(4)	<i>b</i>	<i>b</i>	1.497(4)	1.252(4)	1.289(4)
inner 2	1.397(4)	1.375(4)	1.501(4)	1.488(5)	1.467(5)	1.494(4)	1.256(4)	1.281(4)
outer 1	1.444(5)	1.332(5)	1.480(5)	<i>b</i>	<i>b</i>	1.490(5)	1.214(4)	1.329(4)
outer 2	1.428(4)	1.336(4)	1.499(5)	1.478(5)	1.485(6)	1.511(5)	1.224(4)	1.332(4)
2a (293 K)	1.412(3)	1.356(3)	1.499(4)	1.497(5)	1.500(4)	1.503(4)	1.246(3)	1.303(3)
2b (223 K)	1.423(4)	1.359(5)	1.497(6)	1.495(6)	1.504(6)	1.506(5)	1.237(4)	1.309(4)
4	1.389(9)	1.393(8)	1.490(8)	<i>b</i>	<i>b</i>	1.495(9)	1.258(7)	1.258(7)

^a Values obtained from the Cambridge Structural Database.³⁵ Estimated standard deviations not available. ^b C–C distances could not be determined accurately due to disorder (see Synthesis and Characterization).

Chart 1

The resulting structural unit contains a large, nearly planar system formed by two [(CHD)₄][−] systems and two dibenzene chromium cations (see Figure 3b). The analogy between the structure of **1** and Etter's CHD cyclamer encapsulating a benzene molecule is clear (compare with Figure 1), but, while Etter's cyclamer is composed of neutral components, the organic host and the organometallic guest in **1** have opposite net charge because of the deprotonation of one dione per [(η^6 -C₆H₆)₂Cr]⁺ formula. In **1**, segregation is attained with two [(CHD)₂][(CHD)₂][−] "horseshoes" embracing two [(η^6 -C₆H₆)₂Cr]⁺ ions.

A comparison between Figures 3 and 4 allows one to appreciate the relationship between crystals of the benzene (**1**) and the toluene (**2**) derivatives. In crystalline **2**, the supramolecular [(CHD)₂][−] anion is composed of two hydrogen-bonded CHD systems (see Figure 4a). The O...O separation is comparable to the inner hydrogen bond in **1** [O...O, 2.469(2) and 2.437(5) Å in **1** and **2**, respectively]. The bond length distribution within the CHD system in **2** is clearly indicative of the keto-enol form, the two outer C–O distances being consistently shorter than the two inner ones [C8–O1, 1.246(3) (**2a**) and 1.237(4) (**2a**) Å versus C10–O2, 1.303(3) (**2a**) and 1.309(4) (**2b**) Å]. The C–C bond length distribution is

also in agreement with this bonding picture: C9–C10 [1.356(3) (**2a**) and 1.359(5) (**2b**) Å] shows a clear double bond character, whereas C8–C9 and C10–C11 are slightly longer [1.412(3) and 1.499(4) Å for **2a**; 1.423(4) and 1.497(6) Å for **2b**], and C8–C13, C12–C13, and C11–C12 are much longer [1.503(4), 1.500(4), and 1.497(5) Å for **2a**; 1.506(5), 1.504(6), and 1.495(6) Å for **2b**].

Substitution of one methyl group for a hydrogen atom on the cation changes the overall shape of the fragment. Toluene, with its Me group protruding from one side, is no longer discoidal in shape with respect to benzene. The relatively small *chemical* change on passing from benzene to toluene has dramatic effects on the way these molecules are packed. It is well known, for example, that, while benzene undergoes a facile reorientational jumping motion in its crystal as in all crystals formed by organometallic complexes carrying benzene as a ligand, toluene is blocked in its motion in the solid state.²⁶ Most toluene complexes show that the ligand can undergo, at the most, large-amplitude *swinging* motion but not full-scale reorientation. Since the barrier to *internal rotation* in most bis-arene and metallocenes complexes is very low,²⁷ the rotameric conformations adopted in the solid state by these complexes are often determined by the optimization of intermolecular interactions.²⁶

The different packing requirements of benzene and toluene are obviously reflected in the structures of crystalline **2**. As mentioned above, the bis-toluene cation adopts two different rotameric orientations (conformations A and B, see Figure 2) within the environment provided by the dimeric monoanions [(CHD)₂][−] in the crystal packing. Isomer A is probably better suited to pack with the V-shaped [(CHD)₂][−] anion (see Figure 4b) than isomer B. Figure 5 shows a comparative view of the two *alternative* sets of inter-ion C–H...O hydrogen bonds established by the bis-toluene complex in either conformation with the surrounding [(CHD)₂][−] anions. Though via different donor–acceptor pairs, the overall contribution of C–H...O bonds to crystal cohesion is preserved (see Table 4).

(26) Braga, D. *Chem. Rev.* **1992**, *92*, 633.

(27) Muettterties, E. L.; Bleeke, J. R.; Wucherer, E. J.; Albright, T. A. *Chem. Rev.* **1982**, *82*, 499.

Table 4. Relevant Hydrogen Bonding Parameters (Distances are in Å and Angles in Degrees)

contact type	1	2b (223K)	3	4
O...O	O _{CHD} ...O _{CHD}	O _{CHD} ...O _{CHD}	O _w ...O _w	O _w ...O _w
	2.469(2) 2.544(2) 2.570(2)	2.437(5)	2.815(4) 2.963(4) 2.967(4) 2.985(4)	2.742(6) 2.758(6) 2.784(6)
CH...O	H _{benz} ...O _{CHD}	H _{tol} ...O _{CHD}	H _{benz} ...O _w	O _{CHD} ...O _w
	2.370(4) 2.595(4) 2.409(4) 2.389(4) 2.682(4) 2.288(4) 2.637(4) 2.649(4) 2.553(4) 2.446(4)	2.335(3) ^a 2.385(3) ^a 2.344(3) ^a 2.417(3) ^a 2.521(3) ^b 2.568(3) ^b 2.324(3) ^b	2.63(2) 2.60(2)	2.754(5) 2.770(5) 2.764(5) 2.668(7) 2.675(7) 2.620(7) 2.506(7) 2.635(7) 2.623(7) 2.578(7)
	C-H...O	C-H _{benz} ...O _{CHD}	C-H _{tol} ...O _{CHD}	C-H...O _{w/CHD}
	158.7(2) 150.7(2) 152.0(2) 131.3(2) 117.8(2) 173.0(2) 152.0(2) 148.4(2) 141.1(2) 127.3(2)	135.3(4) ^a 155.3(4) ^a 156.2(4) ^a 140.4(4) ^a 137.2(4) ^b 130.0(4) ^b 133.4(4) ^b	142(1) 146(1)	121(1) 138(1) 163(1) 140(1) 122(1) 125(1) 132(1)

^a Conformer A. ^b Conformer B.

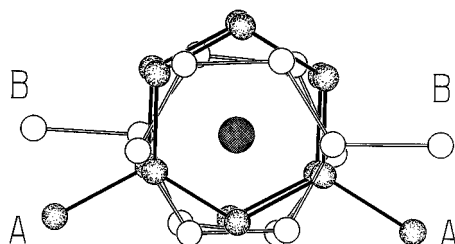


Figure 2. Crystalline **2**. Projections perpendicular to the arene plane show the rotameric 1:1 disorder of $[(\eta^6\text{-C}_6\text{H}_5\text{-Me})_2\text{Cr}]^+$ in crystalline **2**: in conformer A (shaded atoms), the Me groups are at 120° , while in conformer B, they are 180° *trans* with respect to the chromium atom.

Although the crystal structures of $[(\eta^6\text{-C}_6\text{H}_6)_2\text{Cr}][\text{OH}]\cdot 3\text{H}_2\text{O}$ (**3**) and $[(\eta^6\text{-C}_6\text{H}_6)_2\text{Cr}][\text{CHD}]\cdot 3\text{H}_2\text{O}$ (**4**) are related to that of **1**, the participation of water in the construction of the crystals introduces some unique features that make **4** more similar to **3** than to **1** and **2**, although they contain the CHD fragment.

The crystalline organometallic hydrated hydroxide **3** is composed of a stacking sequence (ABABAB) of layers containing $[(\text{C}_6\text{H}_6)_2\text{Cr}]^+$ cations intercalated with layers of water molecules and OH^- groups (see Figure 6a). The $\{[\text{OH}]\cdot 3\text{H}_2\text{O}\}_n$ layer is formed as a slightly puckered hexagonal network containing three water molecules and one OH^- group per formula unit, with the O-atoms hydrogen bonded to three neighbors (see Figure 6b,c). This type of network is present in some inorganic hydroxides²⁸ as well as in some forms of ice.²⁹ The interlayer link is provided by three C-H...O interactions between each crystallographically independent

oxygen atom and the benzene ligands above and below the hydrated layers. In such a way, the "total coordination" around the water (or OH^-) oxygens is given by two donor and one acceptor O-H...O bonds' and by three C-H...O acceptor bonds. The hydrogen bonds distribution around the two crystallographically independent O atoms is shown in Figure 7. The participation of C-H...O interactions in satisfying the hydrogen bond requirements of water molecules has been demonstrated in a survey of hydrated crystals studied by neutron diffraction.³⁰ The presence of a number of H...O(water) interactions higher than the number of available accepting sites (the O atom lone pairs) is indicative of the limited directional requirements of the C-H...O bonds and of their chiefly electrostatic nature. It has been shown that a key role in the hydrogen bonding of water molecules is played by the repulsions between the oxygen atoms.³¹ This is probably the reason why four-fold or higher "coordination" is possible when some of the donors are CH groups, while it is extremely rare with only water donors.

It is worth noting that structure **3** is polar, with the layers stacked along the polar *c*-axis of the *Aba2* space group. The implication of this structural arrangement is remarkable: the (001) faces of the crystal must be formed on one side of a hydrophobic (or only slightly hydrophilic) layer of $[(\text{C}_6\text{H}_6)_2\text{Cr}]^+$ cations packed in herringbone fashion and on the opposite side of a highly hydrophilic $\{[\text{OH}]\cdot 3\text{H}_2\text{O}\}_n$ layer. This means that the interaction of water with these two faces would be very different and that the water layer might provide a template structure for the nucleation of ice. It is well

(28) Wells A. F. *Structural Inorganic Chemistry*; Clarendon Press: Oxford, 1984.

(29) Falk, M.; Knop, O. In *Water. A Comprehensive Treatise*; Franks, F., Ed.; Plenum Press: New York, 1973; Vol. 2, p 55.

(30) Steiner, T.; Saenger, W. *J. Am. Chem. Soc.* **1993**, *115*, 4540. Steiner, T.; Saenger, W. *Acta Crystallogr., Sect. B* **1992**, *B48*, 819.

(31) Bouquiere, J. P.; Finney, J. L.; Savage, H. J. F. *Acta Crystallogr., Sect. B* **1994**, *B50*, 566. Savage, H. F.; Finney, J. L. *Nature* **1986**, *322*, 717.

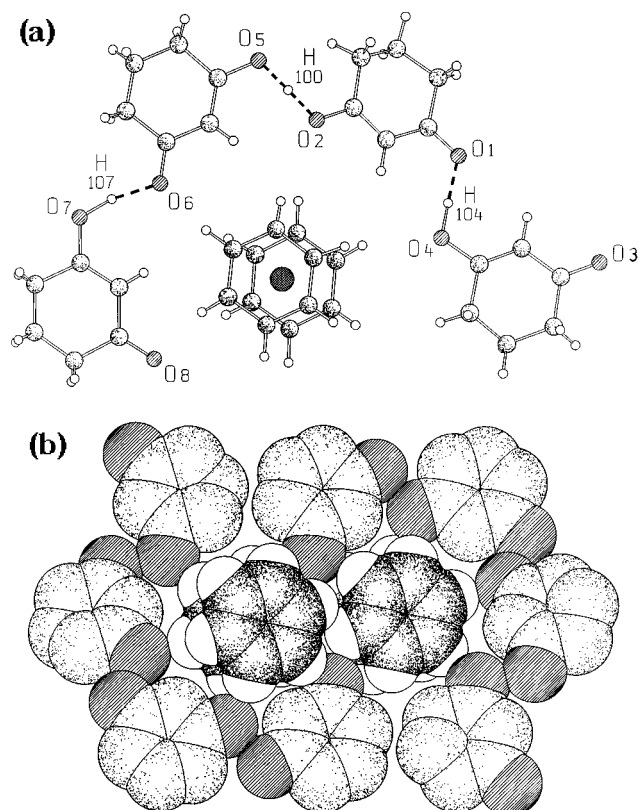


Figure 3. (a) Tetrameric monoanion $[(\text{CHD})_4]^-$ formed by two outer CHD molecules in the keto-enol form and one inner tautomeric pair wrapped around a single $[(\eta^6\text{-C}_6\text{H}_6)_2\text{-Cr}]^+$ ion. Observed H atoms involved in the $\text{O}-\text{H}\cdots\text{O}$ hydrogen bonds are also shown (see text). (b) A centrosymmetric pair of $[(\eta^6\text{-C}_6\text{H}_6)_2\text{Cr}][(\text{CHD})_4]$ showing how eight CHD systems encapsulate two $[(\eta^6\text{-C}_6\text{H}_6)_2\text{Cr}]^+$ cations. Hydrogen atoms of the anions are omitted for clarity.

known that the hexagonal polymorph of AgI promotes ice formation by providing a template lattice. Indeed, Leiserowitz and co-workers³² have shown how a structural match between substrate and the hexagonal lattice of ice may explain the ice nucleation ability of some α -amino acids^{32a} and of two-dimensional long-chain aliphatic alcohols.^{32b}

An additional point of interest in the structure of **3** is that the opposite (001) and (00 $\bar{1}$) faces have opposite charge.

The structure of the hydrated $[\text{CHD}]^-$ salt **4** is strictly related to that of the hydroxide. The CHD system acts as “end caps” of the hexagonal water layers via $\text{O}(\text{water})\text{H}\cdots\text{O}(\text{CHD})$ links; this results in the formation of strings parallel to the a -axis, as shown in Figure 8a. The water molecules, arrangement within the strings is similar to that within the hydrated layers of **3**. The CHD moiety possesses idealized m -symmetry, which probably arises from delocalization of the charge within the $\text{OC}-\text{C}(\text{H})-\text{CO}$ system (see below). Both CHD and water interact with the $[(\text{C}_6\text{H}_6)_2\text{Cr}]^+$ cations via $\text{CH}\cdots\text{O}$ interactions of the type discussed above. The resulting packing arrangement shown in Figure 8b is reminiscent of that shown in Figure 6a, being composed of a stacking sequence of cations and of layers containing water and CHD^- anions.

(32) (a) Gavish, M.; Wang, J.-L.; Eisenstein, M.; Lahav, M.; Leiserowitz, L. *Science* **1992**, *256*, 815. (b) Majewski, J.; Popovitz-Biro, R.; Bouwman, W. G.; Kjaer, K.; Als-Nielsen, J.; Lahav, M.; Leiserowitz, L. *Chem. Eur. J.* **1995**, *1*, 304.

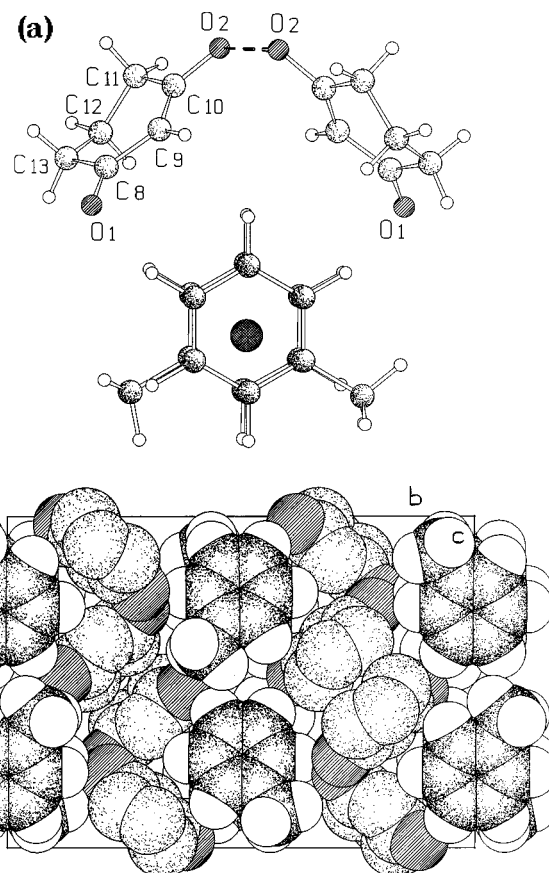


Figure 4. (a) Dimeric monoanion $[(\text{CHD})_2]^-$ formed by two CHD molecules, “clamping” a single $[(\eta^6\text{-C}_6\text{H}_5\text{Me})_2\text{Cr}]^+$ ion (conformer A is shown). A crystallographic two-fold axis passes through the Cr atom and the middle of the intra-CHD hydrogen bond. (b) Space-filling representation of the packing arrangement in crystalline **2** (only conformer A of the disordered toluene ligand is shown). Hydrogen atoms of the anions are omitted for clarity.

It is now possible to draw some conclusions from the structural comparisons:

(i) The 1,3-cyclohexanedione molecule and its deprotonation product are extremely versatile systems that can be combined in a number of different ways to build crystals.

(ii) This capacity arises chiefly from the electronics and bonding of the keto-enol tautomerism that makes CHD adaptable to different intermolecular environments. This is well demonstrated by the data in Table 3 (Chart 1 can be used as reference; subscript numbers in the following discussion refer to the scheme in Table 3). While the bonding within the sequence of sp^3 carbon atoms (atoms 4, 5, and 6 in the Table 3 scheme) is, as expected, affected very little by the change in charge and bonding of the rest of the system, important differences are seen along the sequence $\text{O}_7=\text{C}_1-\text{C}_2=\text{C}_3-\text{O}_8$.

(iii) In both crystalline forms of neutral CHD, the C_2-C_3 distances are significantly shorter than the C_1-C_2 bonds, and the ketonic C_1-O_7 distances are shorter than the enolic C_3-O_8 bonds, indicating a marked difference in bond order.

(iv) In crystalline **1**, the difference between “short” and “long” sets of distances along the sequence $\text{O}_7=\text{C}_1-\text{C}_2=\text{C}_3-\text{O}_8(\text{H})$ is accentuated for the outer and decreased for the inner CHD systems. The increase in bonding localization witnesses the loss of resonance-assisted

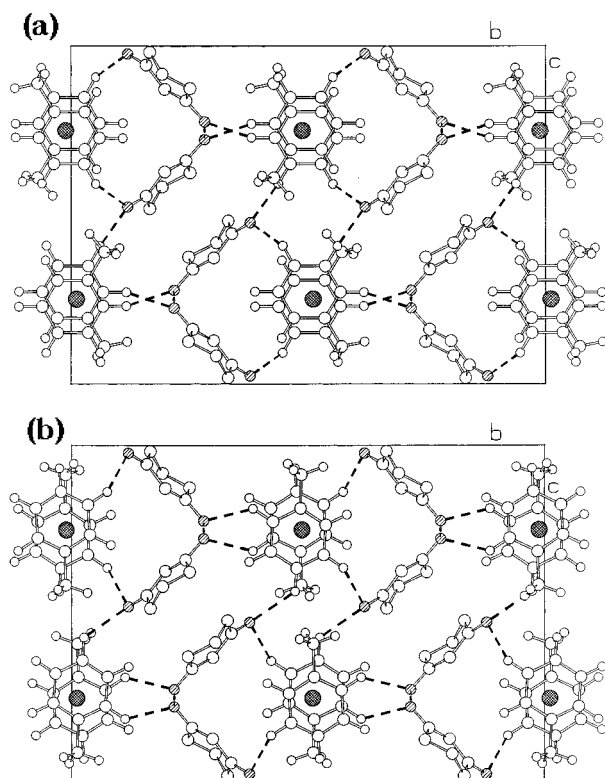


Figure 5. Comparative views of the crystal packing of **2**, showing the most relevant O...HC(toluene) hydrogen bond interactions established by the complex with the surrounding $[(\text{CHD})_2]^-$ anions in conformations (a) A and (b) B, respectively. Hydrogen atoms of the anions are omitted for clarity.

hydrogen bond contribution with respect to the delocalization around the cyclamer and along the molecular rows in crystalline CHD. To the contrary, the removal of one proton between the two inner CHDs in **1** generates a highly delocalized system conjugated through the inner hydrogen bond.

(v) The inner O...O distances in both $(\text{CHD})_2 \cdot [(\text{CHD})_2]^-$ and $[(\text{CHD})_2]^-$ anions are very short; they are much shorter than those observed in both CHD crystal structures (2.561 and 2.579 Å in the chain and cyclamer crystals, respectively). The shortening is well accounted for by the model of negative charge-assisted hydrogen bond put forward by Gilli et al.³³

(vi) The $[(\text{CHD})_2]_2^-$ system in **2** shows a bond length pattern which is intermediate between those of the outer and the inner CHD systems in **1** (see Table 3).

(vii) In crystalline **4**, on the other hand, an extreme bonding delocalization is observed as both C–O bonds and both C–C bonds within the O7=C1–C2=C3–O8 have roughly the same length. This might be taken as indicative that the proton is removed exclusively from the CHD system and not from water, i.e., the crystal is composed of hydrated CHD⁻ anions interacting with the organometallic cations. Interestingly, the structural parameters within the CHD moiety are strictly comparable to those observed in the lithium enolate crystals obtained by Etter from methanol and 2,2,2-trifluoroethanol solutions of Li-CHD (see Table 3).³⁴ In both structures, the C–O as well as the inner C–C bonds have almost equal length, viz., removal of the enol

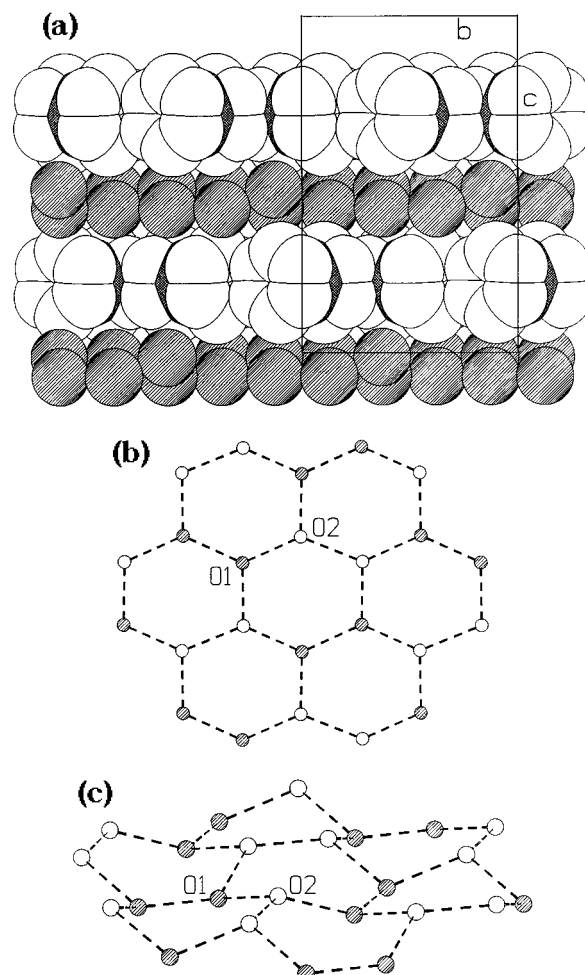


Figure 6. (a) ABABAB stacking sequence of layers in crystalline **3** formed by $[(\text{C}_6\text{H}_6)_2\text{Cr}]^+$ cations intercalated with layers of $\{[\text{OH}] \cdot 3\text{H}_2\text{O}\}_n$. Hydrogen atoms are omitted for clarity. A projection (b) and a side view (c) of the $\{[\text{OH}] \cdot 3\text{H}_2\text{O}\}_n$ layer show the puckering of the hexagonal network (the two crystallographically independent oxygens O1 and O2 are represented as dashed and empty spheres).

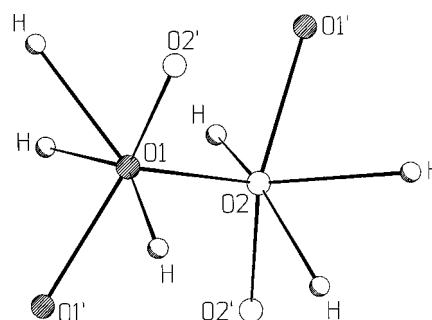


Figure 7. Hydrogen bond coordination around the two independent oxygen atoms in crystalline **3**. Note how each oxygen atom participates in three O...O and three O...H-C hydrogen bonds.

proton leads to complete delocalization in the solid state, exactly as observed in structure **4**. However, it may be argued that the same bond length pattern in **4** can arise from static disorder, i.e., as a result of an *average over space* of CHD in keto-enol form as in **1** and **2**.

(34) Etter, M. C.; Ranawake, G. *J. Am. Chem. Soc.* **1992**, *114*, 4430.

(35) Allen, F. H.; Davies, J. E.; Galloy, J. J.; Johnson, O.; Kennard, O.; Macrae, C. F.; Watson, D. G. *J. Chem. Inf. Comput. Sci.* **1991**, *31*, 204.

(33) Gilli, P.; Bertolasi, V.; Ferretti, V.; Gilli, G. *J. Am. Chem. Soc.* **1994**, *116*, 909.

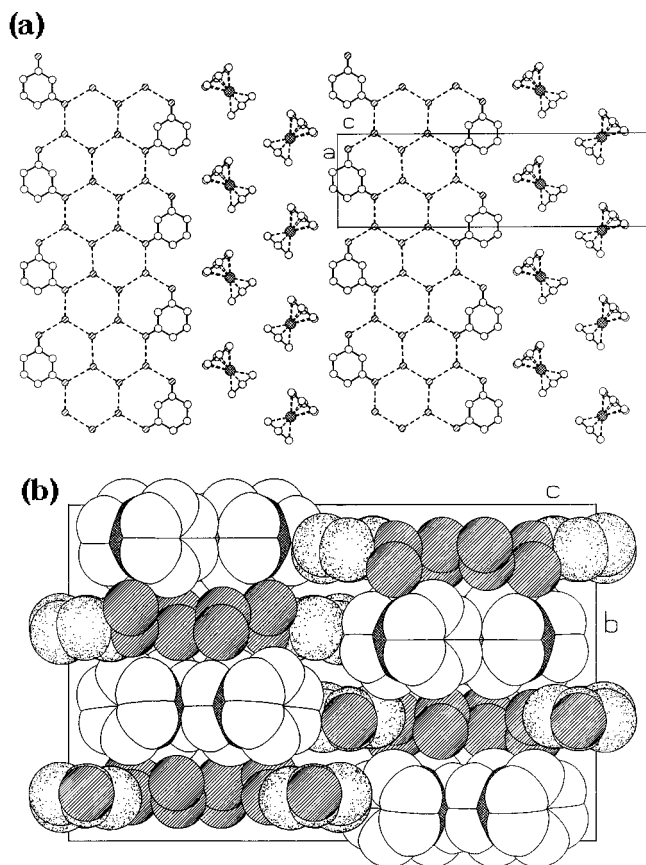


Figure 8. Crystalline $[(\eta^6\text{-C}_6\text{H}_6)_2\text{Cr}][\text{CHD}]\cdot 3\text{H}_2\text{O}$ (**4**). (a) Projection in the ac -plane showing how the $[(\eta^6\text{-C}_6\text{H}_6)_2\text{Cr}]^+$ cations are intercalated with strings of $[\text{CHD}]\cdot 3\text{H}_2\text{O}$ extending along the a -direction. Hydrogen atoms are omitted for clarity. (b) Space-filling outline of the projection in the bc -plane.

(viii) Some insight into the disorder problem comes from the information on hydrogen bond lengths listed in Table 4. The difference in $\text{O}\cdots\text{O}$ separation between water/ OH^- oxygens in the hydroxide **3** and in the hydrated crystal **4** is substantial (mean 2.93_8 versus 2.760_{15} Å). Longer $\text{O}\cdots\text{O}$ separations in the hydroxide are in keeping with the presence of repulsive $\text{O}\cdots\text{O}$ electrostatic interactions within the $\{[\text{OH}]\cdot 3\text{H}_2\text{O}\}_n$ layer. Although OH^- should form stronger hydrogen bonds with water than water itself, one OH^- ion for every three water molecules is not sufficiently *diluted*, and the $\text{O}\cdots\text{O}$ separation results as a compromise between hydrogen-bonding optimization and minimization of $\text{OH}\cdots\text{OH}^-$ repulsions. In **4**, where the charge is localized on the CHD system, the approach between the water oxygens increases.

(ix) This description of the participation of water in hydrogen bonding is in agreement with the structural parameters available for the various forms of ice, where $\text{O}\cdots\text{O}$ distances are in the range $2.752\text{--}2.800$ Å.²⁸

Conclusions and Perspectives

The idea of constructing crystalline materials with predefined molecular arrangements is attracting much interest in these days of supramolecular and materials chemistry. The main outcome of this study is, indeed, the design of organic–organometallic supramolecular aggregates which carry in the solid state the paramagnetic cations $[(\eta^6\text{-arene})_2\text{Cr}]^+$ (arene = benzene and

toluene) via hydrogen bonds of different nature. The aggregation of the CHD systems in superanions and/or in extended aggregates linking water is based on strong hydrogen bonds, whereas the interaction between organic aggregates and organometallic complexes is essentially based on weak $\text{C}\text{--}\text{H}\cdots\text{O}$ hydrogen bonds, reinforced by the different polarity. The organization in the crystal of the benzene cyclamer is similar to that observed in **1** because of the *shape analogy* between benzene and bis(benzene)chromium. However, as the shape of the guest cation is changed on going from $[(\text{C}_6\text{H}_6)_2\text{Cr}]^+$ to $[(\text{C}_6\text{H}_5\text{Me})_2\text{Cr}]^+$, an efficient “embrace” by a large CHD oligomer or cyclamer is no longer possible.

Besides reporting the results of crystal synthesis, the objective of this paper is also to demonstrating the enormous potential of organic–organometallic crystal engineering as a means of *combining* structural and chemical features of molecules in the two fields. In spite of these differences, the major cohesive interactions present in Etter’s cyclamer and in **1** and **2**, i.e., hydrogen bonds of both $\text{O}\text{--}\text{H}\cdots\text{O}$ and $\text{C}\text{--}\text{H}\cdots\text{O}$ types, are maintained in the different crystalline edifices. Hence, $\text{O}\text{--}\text{H}\cdots\text{O}$ and $\text{C}\text{--}\text{H}\cdots\text{O}$ hydrogen bonds afford a pattern of interactions in common between organics, organometallics, and water that can be utilized to engineer crystalline materials based on the complementarity between donors and acceptors. The third partner, water or other solvent molecules, can also be varied.

The crystal of the hydroxide **3** constitutes a remarkable example of the supermolecule crystal analogy: the noncovalent aggregation of water and two simple ions such as OH^- and $[(\text{C}_6\text{H}_6)_2\text{Cr}]^+$ generates a highly specialized superstructure in which layers of opposite sign alternate and result in a system with *sides* of completely different chemical composition and, therefore, of presumably different physical and chemical properties.

This type of approach has many possible applications. Indeed, the same way of thinking can be extended to other systems such as *bioorganometallic* crystal engineering: for example, the interaction between metal complexes and natural aminoacids may be exploited to build new aggregates in chiral space groups. Initial results are very promising. Furthermore, the study of the interaction of water in organometallic crystals can reveal some new interesting features of the interaction of water with the surroundings.

Acknowledgment. The ERASMUS program “Crystallography”, the Deutscher Akademischer Austauschdienst, Bonn, and the Conferenza Nazionale dei Rettori, Roma, are thanked for scientific exchange grants. Janice Byrne, Stefan Gebert, Andreas Wolf, and Douglas Shephard are thanked for their help at various stages of this work. Professors Achille Umani Ronchi (Bologna) and Fausto Calderazzo (Pisa) are thanked for useful suggestions and encouragement. Financial support by M.U.R.S.T. and by the University of Bologna (project: Intelligent molecules and molecular aggregates) is acknowledged.

Supporting Information Available: Tables of anisotropic thermal parameters and fractional atomic coordinates, complete lists of bond lengths and angles, and ORTEP drawings (43 pages). Ordering information is given on any current masthead page.

OM9603878